Estimating Carbon Sequestration Potential in Vegetation by Distance-Constrained Zonal Analysis

Zongyao Sha, Ruren Li, Jonathan Li, *Senior Member, IEEE*, and Yichun Xie, *Member, IEEE*

***Abstract*— This letter proposes a distance-constrained (DC) zonal analysis approach to quantify how much more carbon could be further sequestrated by vegetation in mainland China based on multiple data sources. Our approach first segments the area into homogeneous landform–vegetation–soil (LVS) zones. Good land management practice (GLMP) corresponding to high sequestrated carbon (target carbon level) is identified at the locations in the same LVS zone. The target carbon level is set as the 90th percentile of the historically sequestrated carbon using the proxy of net primary productivity (NPP) at the locations within the LVS zone. When GLMP is realized over the entire LVS zone, more carbon could be sequestrated. Our results show that on average about 1/4 of more carbon could be added to the existing amount given the selected "good" land management practices are adopted by neighboring locations where lower carbon sequestration levels exist. The carbon sequestration potential for different land cover types differs significantly.**

***Index Terms*— Carbon sequestration, Google Earth Engine (GEE), land management, remote sensing, vegetation, zonal analysis.**

I. Introduction

GLOBAL warming due to increased emissions of carbon dioxide (CO_2) and other greenhouse gases into the atmosphere has called for an urgent response to moderate possible ways to stop the continually rising global temperature, which is extensively debated among academicians and governmental agencies [1]–[3]. Limiting carbon fuel consumption and its atmospheric output, as a direct measure, has been proposed for decades, but the implementation of the proposal has not been widely recognized due to the fact that the current economy in many countries is powered by fossil fuels [4], [5]. Applying a biotic strategy to sequestrate more atmospheric CO_2 provides a promising method to respond to global warming [6]. Vegetation-dominated terrestrial ecosystems, including forests, grasslands, croplands, shrublands, or savannas, absorb substantial greenhouse gases from the atmosphere through a carbon sequestration process called photosynthesis [7], [8]. The factors affecting carbon sequestration include climate, landform variations [9], vegetation cover [10], land cover/use patterns [11], and natural environmental conditions such as soil properties [12], [13]. The amount of sequestrated carbon is changeable depending on those factors. Precipitation and temperature, for example, have been found to closely link to carbon sink from vegetation [14]–[16].

Human-related land/vegetation management practices such as land conservation [17], rotation [18], irrigation/drainage [19], fertilization, or tillage [20] can alter vegetation health and thus recuperate carbon sequestration. Converting land cover from agricultural land to forestry can promote vegetation cover density and help sequestrate more carbon [21]. However, the conversion of economic land use to natural land cover is not readily implementable due to the concerns from socioeconomic development, for example, food production. Thus, it is more advisable to resolve other inexpensive strategies for decreasing the CO_2 level in the atmosphere [22].

The carbon sequestration potential can be assessed in a variety of methods. First, carbon sequestration potential may be realized by land cover conversions. However, strengthening carbon sequestration through land cover conversions is of limited value because such practices are restrained by other factors and land covers might not be freely convertible. Second, the carbon potential can be estimated by projecting future climate changes. Carbon sequestration from vegetation could increase from 1/5 to 1/3 under a few scenarios of climate changes [15]. The future climate projection methods inherit some critical uncertainties from the projected climate data, and thus provide limited value for policy-making at current. Relying on the power of human intervention to improving climatic conditions seems unreasonable especially within a short period. Third, carbon potential could be assessed by differential analysis between the potential carbon sequestration level and its current level [23]. In such models, the theoretical carbon level defines the maximum value of carbon that vegetation can sequester. However, it is unknown whether the potential could be really reached given that the vegetation growth is constrained from varieties of environmental conditions.

This letter proposes a distance-constrained (DC) zonal analysis to assess carbon sequestration potential. This model assesses how much more carbon (carbon gap hereafter) could

Manuscript received April 4, 2020; revised May 31, 2020; accepted June 15, 2020. This work was supported in part by the National Natural Science Foundation of China under Grant 41871296 and Grant 51774204. *(Corresponding author: Yichun Xie.)*

Zongyao Sha is with the School of Remote Sensing and Information Engineering, Wuhan University, Wuhan 430079, China (e-mail: zongyaosha@whu.edu.cn).

Ruren Li is with the College of Transportation, Shenyang Jianzhu University, Shenyang 110044, China (e-mail: cerrli@sjzu.edu.cn).

Jonathan Li is with the Department of Geography and Environmental Management, University of Waterloo, Waterloo, ON N2L3G1, Canada (e-mail: junli@uwaterloo.ca).

Yichun Xie is with the Department of Geography and Geology, Eastern Michigan University, Ypsilanti, MI 48197 USA (e-mail: yxie@emich.edu).

Color versions of one or more of the figures in this letter are available online at http://ieeexplore.ieee.org.

Digital Object Identifier 10.1109/LGRS.2020.3003448

be sequestered by evaluating the influence of human-related land management practice. The model also outputs the areas showing the most sensitive to land management optimization in terms of the space in extra carbon sequestration. The result from the assessment provides ready-to-implement policy decision guidance in response to future climate changes.

II. Study Area and Data

A. Study Area

The mainland China has been selected as the study area. According to the International Geosphere-Biosphere Programme (IGBP) land cover classification system, there are 17 classes, of which 13 are closely related to vegetation cover types [except for 13. Urban and built-up lands, 15. Snow and ice, 16. Barren, and 17. Water bodies]. Thus, the 13 land cover classes play a vital role in sinking CO_2 from the atmosphere. The carbon gap for the whole region and for each land cover type is highlighted by the proposed model.

B. Data

The majority of the data sources come from Google Earth Engine (GEE) and all the computing processes are based on the GEE platform. There are three groups of data sources involved, namely, climate-related variables, nonclimate variables, and net primary productivity (NPP). Those data sets, if not at the scale of 500 m, will uniformly be resampled to a resolution at 500 m.

Precipitation and temperature are the most important elements in the climate-related variables because both of them were confirmed to alter NPP and thus carbon uptake [23]. Theoretical NPP has been modeled purely from climatic conditions; the empirical Miami model is considered to be the first one that computes potential NPP (PNPP) using monthly precipitation and temperature and often used as a baseline for model comparison [24]. TerraClimate derived from climatically aided interpolation by combining WorldClim and Climate Research Unit (CRU) data set has been widely applied for mapping regional and global ecological parameters [25] and is used to assess the variation in the climate impact on observed NPP (ONPP). It contains monthly precipitation and maximum and minimum temperatures at the spatial resolution of 2.5 arcmin.

Nonclimate variables include soil type, landform, and vegetation type. Soil type strongly affects the vegetation growth and is included as a key element in the nonclimate group. Harmonized World Soil Database (www.fao.org/soils-portal) is the most up-to-date world soil map which incorporates a data table of 48 148 soil profile descriptions related to the various soils associated with each mapping unit, at a spatial resolution of about 1 km [26]. Soil type class using FAO-90 code is used as the soil mapping unit. A region covered by the same soil type is believed to have a limited internal variation in the soil property. The topography is found to affect vegetation NPP [27]. Landform cover, as a comprehensive indicator of topographic attributes, is taken as the second nonclimate element. Landform cover from European Soil Data Centre (https://esdac.jrc.ec.europa.eu) is used, which is dynamically classified using an unsupervised nested-means algorithm based on three geometric signatures (slope, surface texture, and local convexity) from SRTM30 Digital Elevation Model (DEM) [28]. Finally, IGBP land cover from MODIS MOD12Q1 is taken to map vegetation distribution.

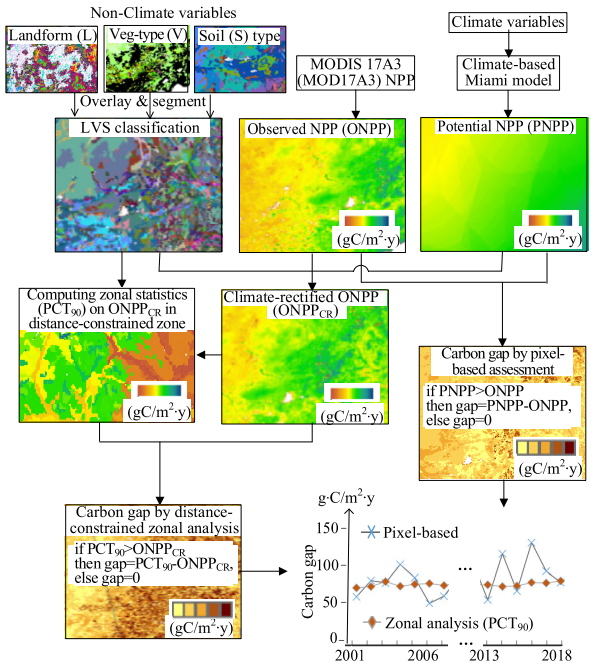

Fig. 1. Flowchart of assessing carbon gap by DC zonal analysis. Spatiotemporal dynamics of carbon gap achieveable by adjusting human-related practices from distance-constrained (DC) zonal analysis as opposed to that by pixel-based assessment.

NPP data set provides a direct indicator of carbon sequestration from vegetation. The MODIS MOD17A2H product (V6) is a cumulative eight-day composite at 500-m spatial resolution. The data set includes time series of net photosynthesis, an indicator of NPP that reflects the spatiotemporal variations in vegetation carbon uptake. The product is based on a wide range of observed parameters (e.g., normalized difference vegetation index) and radiation-use efficiency modeling. Annually accumulated NPP from MOD17A2H is referred to as ONPP hereafter.

III. Method

A. Workflow Description

The factors affecting carbon sequestration from vegetation can be broadly grouped as the following three categories: 1) climate impact (including precipitation and temperature); 2) human-related land-use practices (HUMAN); and 3) other nonclimatic (nonclimate) environmental conditions such as soil property, landforms, and vegetation types. DC zonal analysis isolates the impact of both climate and nonclimate and quantifies the impact on vegetation carbon sequestration from HUMAN. Fig. 1 shows the workflow to assess the achievable carbon gap.

First, region segmentation is performed to derive homogeneous zones in terms of landform, vegetation, and soil type cover so that the internal ONPP variation within an LVS zone due to nonclimatic factors will be minimized, meaning that there is no within-zone ONPP variation from nonclimate impact. Furthermore, climatic factors also affect

ONPP variation in an LVS zone. To offset the climate impact, we apply PNPP, which captures the climate difference based on the climate-driven Miami model, to rectify the impact of climate variations on ONPP. Within each LVS zone, the spatial variation in the climate-rectified ONPP (ONPP_{CR}) will be attributed solely to HUMAN variation because both climate and nonclimate impact has been accounted for. We then apply DC zonal analysis to estimate the carbon gap for all locations (pixels) controlled by the LVS zones.

B. Region Segmentation and ONPP

To account for the spatially varied nonclimate impact on ONPP, the landform (L), vegetation (V) cover, and soil (S) type layers are taken as the key environmental factors, geo-registered to World Geodetic System (WGS)-84, and overlaid to segment the study region into areal patches (landform–vegetation–soil (LVS) units). LVS units labeled by the same LVS# are featured by identical nonclimate conditions. ONPP variation within LVS units having the same LSV label (referred as LVS group/zone hereafter) is thus attributed to differed climate and HUMAN impacts. To further discriminate varied climate impact on ONPP in an LVS group, PNPP, which is mapped by the Miami model, is applied to derive a location-dependent relative contribution (RC) value from the climate impact. The Miami NPP model takes the form [23]

$$\text{PNPP} = \lambda \times \min\{3000/(1+e^{1.315-0.119t}), 3000 \times (1-e^{-0.000664p})\} \quad (1)$$

where t is the annual average temperature (°C), p is the annual precipitation (mm), min is a function that selects the minimum value from the two values in the brackets, and λ is the conversion coefficient (0.50 for woody ecosystems and 0.45 for herbaceous) that converts dry matter into carbon unit ($\text{gC/m}^2\text{/yr}$). RC at location i in an LVS group g is defined as the difference between PNPP at location i and the averaged PNPP of g

$$\text{RC}(i,g) = \text{PNPP}(i,g) - \text{PNPP}_{\text{Mean}}(g) \quad (2)$$

where $\text{PNPP}_{\text{Mean}}(g)$ in (2) is the mean PNPP of all locations in g, PNPP(i,g) is PNPP at i in g, and $\text{RC}(i,g)$ is the difference between PNPP at i and the mean PNPP in g [i.e., $\text{PNPP}_{\text{Mean}}(g)$] due to within-group variation in the climate impact. Clearly, more favorable climate conditions will result in positive and higher PNPP and vice versa. The NPP difference due to the climate variations can be reflected from RC at each location in an LVS group. To offset the difference in the climate impact within an LVS group g, ONPP_{CR} at location i in g can be derived using the function

$$\text{ONPP}_{\text{CR}}(i,g) = \text{ONPP}(i,g) - \text{RC}(i,g). \quad (3)$$

The internal variation in ONPP_{CR} in an LVS group is attributed to HUMAN impact only.

C. Carbon Gap by DC Zonal Analysis

Zonal analysis can derive a set of statistics (e.g., maximum or minimum value) from the input values of a variable within a zone. The carbon gap for a given location is computed as the difference from its current ONPP_{CR} to a target value that could be realistically achieved. For any given location i, such a target value is derived by zonal analysis on ONPP_{CR} input within the colocated LVS zone containing i and a predefined window centered at i, or termed as DC neighborhood. In this study, a zonal statistic, defined as the 90th percentile (PCT_{90}) from the input vector of ONPP_{CR} (ONPP_{CR} values) located in the DC neighborhood, is computed as the target level for ONPP_{CR} at each location.

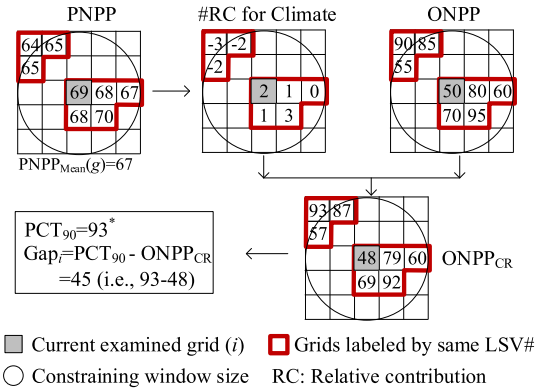

Fig. 2. Example of carbon gap assessment by DC zonal analysis. $^{\#}\text{RC}(i,g) = \text{PNPP}(i,g) - \text{PNPP}_{\text{Mean}}(g)$ and $\text{ONPP}_{\text{CR}}(i,g) = \text{ONPP}(i,g) - \text{RC}(i,g)$, where i means the current examined grid (pixel) and g is the group of the eight grids in the red boundaries [see (2) and (3)]. $^{*}\text{PCT}_{90}$ is computed by DC zonal analysis on ONPP_{CR}; in this example, 93 is the PCT_{90} of the eight ONPP_{CR} values.

The assessment of the carbon gap by DC zonal analysis depends on computing the target reference for a location that its ONPP_{CR} can reach. Two parameters, namely, a zonal statistic and a window size defining the zone, have to be predefined for the analysis. A few zonal statistics could be considered. For example, the maximum zonal statistic from the ONPP_{CR} inputs of a zone is the highest ONPP_{CR} that corresponds to the good land management practice (GLMP) leading to the maximum ONPP_{CR}. GLMP can then be adopted by all other locations, resulting in the highest overall ONPP_{CR} in the LVS zone. Rather than taking the maximum statistic, our selection of PCT_{90} is decided to remove few exceptional ONPP_{CR} values possibly introduced from noisy data (e.g., LVS input or ONPP), which might not be resulted from HUMAN impact. Instead, using PCT_{90} as the target is likely to exclude such exceptions and will provide a more robust reference that ONPP_{CR} is expected to reach if GLMP from the neighborhood is transferred to the currently examined location.

The window size is another parameter that given a location i in an LVS zone constrains the input of ONPP_{CR} from the full LVS zone to only a local window during computing the target ONPP_{CR} for the location. This modification makes sure that only HUMAN practices at locations close to i will be referred to as the candidate for GLMP. The sensitivity of PCT_{90} to the window size, defined as PCT_{90} changes along a series of varied window sizes, is mapped. A stratified random selection of 5000 points, with the sample size allocated by the area of each vegetation type, found that the window size for the peak PCT_{90} was less than 20 km. In the end, the widow size is decided to be 20 km. Fig. 2 shows the steps of an example assessing the carbon gap by DC zonal analysis.

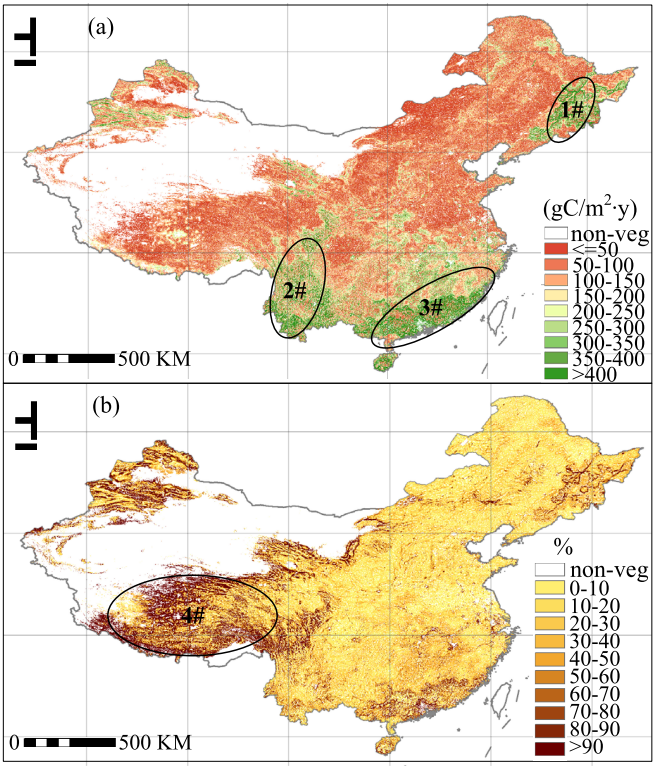

Fig. 3. Distribution patterns of the carbon gap from the DC zonal analysis. (a) Carbon gap flux. (b) Ratio of the carbon gap flux to ONPP (%).

For the location (gray grid) under examination, a 3 × 3 sized window is used to confine the underlying LVS zone, leaving only eight grids (within the red boundaries) as the input for deriving the target $ONPP_{CR}$ from the DC zone. All the other grids intersecting and located in the circular window without filled numbers indicate that they do not have the same LVS label as that of the currently examined grid and thus are not used for computing PCT_{90} (because they belong to another LVS zone). The RC from the climate impact is derived from the PNPP. $ONPP_{CR}$ is obtained by offsetting RC from ONPP. In the end, the zonal statistic, PCT_{90}, is derived and the carbon gap for the location is assessed.

IV. Results and Discussion

Fig. 3 shows the spatial variation in the carbon gap (flux) and the ratio of the carbon gap to ONPP from DC zonal analysis. The total carbon gap flux/density showed highest in the north-eastern part (1#) which was dominated by deciduous broadleaf forests and southern China (2# and 3#) where the land cover types were much complex [Fig. 3(a)]. The relative carbon gap, defined as the ratio (or gap ratio) of the carbon gap to ONPP at each location, presented a different distribution pattern to the carbon gap flux. For example, the west-southern part of the study area (4#), most of which was covered by grassland on high elevation mountains, demonstrated peak ratio value [Fig. 3(b)]. The grassland in the northern China, however, did not show a high relative carbon gap, indicating that the carbon gap varied not only between vegetation cover types but also with other nonclimate environments (e.g., landforms). The carbon gap distribution helps locate the

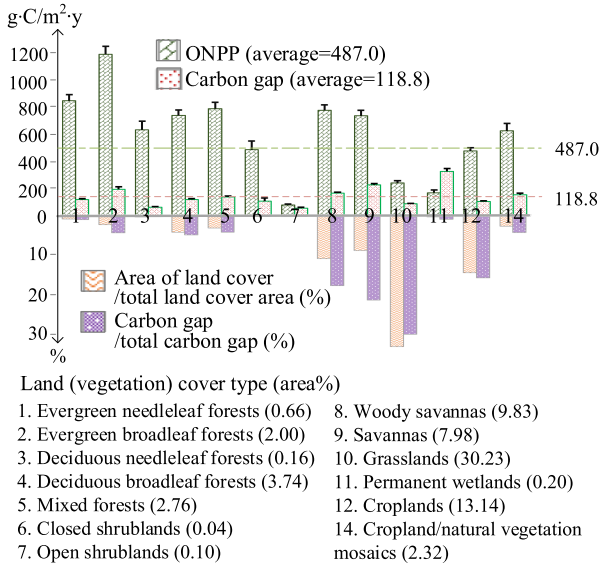

Fig. 4. Carbon gap statistics (mean with error bar from standard deviation) for different land (vegetation) cover types during 2001–2018.

regions where more carbon could be sequestrated from vegetation cover by simply updating HUMAN practices without converting land cover types. Fig. 4 shows the carbon gap statistics on land cover types during 2001–2018.

After excluding the nonvegetated areas, the 13 vegetation cover types averaged an ONPP density of 487.0 gC/m^2/yr, although a significant difference was observed between them. The average carbon gap flux for all the 13 land cover types was 118.8 gC/m^2/yr, suggesting the potential of adding about 1/4 of extra carbon uptake on the existing ONPP. Evergreen broadleaf forests showed the highest ONPP (1166.8 gC/m^2/yr); however, its carbon gap density was only 187.2 gC/m^2/yr (gap ratio = 16%). Permanent wetlands presented the highest carbon gap flux, reaching up to 316.3 gC/m^2/yr, in contrast to its low ONPP which was less than 200 gC/m^2/yr, suggesting the high sensitivity of wetlands to HUMAN impact. Grasslands occupied the largest land area, totaling 30.23% out of all. Grassland averaged an ONPP density of 231.9 gC/m^2/yr, much lower than that of evergreen broadleaf forests. The carbon gap density from grasslands was only 81.5 gC/m^2/yr on average with a much higher gap ratio of 35% than that of evergreen broadleaf forests. The total carbon gap from grasslands took 26.87% of all, significantly higher than that of any others. Savannas and woody savannas took the second-largest potential to capture more carbon given their relatively high gap flux (219.3 and 157.6 gC/m^2/yr, respectively) and high ratio of the land cover area (7.98% and 9.83%), reaching up to 19.08% and 16.89% out of the total carbon potential, respectively. Cropland occupied 13.14% of the total land area, the second-largest following grasslands. The potential to capturing more carbon from croplands is substantial, totaling 14.00% out of all the carbon gap. Because of the small land cover area, the total carbon gap from deciduous needle leaf forests, shrublands (open and closed), and permanent wetlands was minimal.

Intensive verification of the carbon gap is limited due to data unavailability. Nevertheless, we found that the carbon gap

is fairly consistent ($R^2 = 0.37$) with the improvement space of above-ground biomass (AGB) computed from on-site data comparably collected outside of and within over 400 protected vegetation areas across the grassland in Inner Mongolia, China, where long-term fencing and grazing exclusion programs were implemented in the past two decades. The AGB outside the fenced areas experienced HUMAN impact showing significant gap compared with that of the fenced areas where the HUMAN impact was excluded. Future work needs to focus more on direct verification of the carbon gap.

V. Conclusion

This letter has proposed a model called DC zonal analysis to assess how much more carbon could be practically captured from vegetation by improving human-related (HUMAN) land management practices supported by multiple remote sensing data sources. Our model differs from any of the existing ones in that the proposed model maps the potential that could be realistically sequestrated simply by identifying and adopting GLMP from the neighborhood with similar environmental properties. ONPP variations come from three aspects, that is, climate, nonclimate, and HUMAN impact. The spatial variation in ONPP, after leveling off the impact from the climate and nonclimate, is attributed solely to HUMAN difference. Thus, the HUMAN practices proved to have historically produced high $\mathrm{ONPP_{CR}}$ could be copied to locations showing a lower $\mathrm{ONPP_{CR}}$ and with comparable environmental conditions. DC zonal analysis is applied to compute the $\mathrm{PCT_{90}}$ that $\mathrm{ONPP_{CR}}$ expects to reach for segmented zones having similar environmental conditions within a distance of 20 km.

The computed carbon gap illustrates that on average, about 1/4 of carbon is expected to be added to the current carbon sequestration level if identified GLMP is implemented at all respective locations where vegetation does not sequester full carbon of the target level. Grassland had the highest potential for capturing more carbon, followed by savannas (including woody savannas) and cropland. The study also located the most sensitive regions that have the most potential space of carbon sequestration improvement.

References

[1] M. L. Khandekar, T. S. Murty, and P. Chittibabu, "The global warming debate: A review of the state of science," *Pure Appl. Geophys.*, vol. 162, nos. 8–9, pp. 1557–1586, Aug. 2005.

[2] P. B. Holden *et al.*, "Climate–carbon cycle uncertainties and the Paris Agreement," *Nature Climate Change*, vol. 8, no. 7, pp. 609–613, Jul. 2018.

[3] J. Ou, X. Liu, X. Li, and X. Shi, "Mapping global fossil fuel combustion CO_2 emissions at high resolution by integrating nightlight, population density, and traffic network data," *IEEE J. Sel. Topics Appl. Earth Observ. Remote Sens.*, vol. 9, no. 4, pp. 1674–1684, Apr. 2016.

[4] R. Gunderson, D. Stuart, and B. Petersen, "The fossil fuel industry's framing of carbon capture and storage: Faith in innovation, value instrumentalization, and status quo maintenance," *J. Cleaner Prod.*, vol. 252, Apr. 2020, Art. no. 119767.

[5] A. Baranzini, J. C. J. M. van den Bergh, S. Carattini, R. B. Howarth, E. Padilla, and J. Roca, "Carbon pricing in climate policy: Seven reasons, complementary instruments, and political economy considerations," *Wiley Interdiscipl. Rev., Climate Change*, vol. 8, no. 4, p. e462, Jul. 2017.

[6] E. Yan, H. Lin, G. Wang, and H. Sun, "Improvement of forest carbon estimation by integration of regression modeling and spectral unmixing of Landsat data," *IEEE Geosci. Remote Sens. Lett.*, vol. 12, no. 9, pp. 2003–2007, Sep. 2015.

[7] R. Lal *et al.*, "The carbon sequestration potential of terrestrial ecosystems," *J. Soil Water Conserv.*, vol. 73, no. 6, pp. 145A–152A, 2018.

[8] M. L. Imhoff, L. Bounoua, T. Ricketts, C. Loucks, R. Harriss, and W. T. Lawrence, "Global patterns in human consumption of net primary production," *Nature*, vol. 429, no. 6994, pp. 870–873, Jun. 2004.

[9] J. E. M. Baartman, A. J. A. M. Temme, and P. M. Saco, "The effect of landform variation on vegetation patterning and related sediment dynamics," *Earth Surf. Processes Landforms*, vol. 43, no. 10, pp. 2121–2135, Aug. 2018.

[10] Y. Liu, G. Yu, Q. Wang, Y. Zhang, and Z. Xu, "Carbon carry capacity and carbon sequestration potential in China based on an integrated analysis of mature forest biomass," *Sci. China Life Sci.*, vol. 57, no. 12, pp. 1218–1229, Dec. 2014.

[11] C. Gang, W. Zhao, T. Zhao, Y. Zhang, X. Gao, and Z. Wen, "The impacts of land conversion and management measures on the grassland net primary productivity over the Loess Plateau, Northern China," *Sci. Total Environ.*, vol. 645, pp. 827–836, Dec. 2018.

[12] Y. Zhang, K. Huang, T. Zhang, J. Zhu, and Y. Di, "Soil nutrient availability regulated global carbon use efficiency," *Global Planet. Change*, vol. 173, pp. 47–52, Feb. 2019.

[13] L. A. Jones *et al.*, "The SMAP level 4 carbon product for monitoring ecosystem land-atmosphere CO_2 exchange," *IEEE Trans. Geosci. Remote Sens.*, vol. 55, no. 11, pp. 6517–6532, Nov. 2017.

[14] G. S. Solangi, A. A. Siyal, and P. Siyal, "Spatiotemporal dynamics of land surface temperature and its impact on the vegetation," *Civil Eng. J.*, vol. 5, no. 8, pp. 1753–1763, Aug. 2019.

[15] E. Dai, Y. Huang, Z. Wu, and D. Zhao, "Analysis of spatio-temporal features of a carbon source/sink and its relationship to climatic factors in the inner Mongolia grassland ecosystem," *J. Geographical Sci.*, vol. 26, no. 3, pp. 297–312, Mar. 2016.

[16] P. Fu, "Responses of vegetation productivity to temperature trends over continental United States from MODIS imagery," *IEEE J. Sel. Topics Appl. Earth Observ. Remote Sens.*, vol. 12, no. 4, pp. 1085–1090, Apr. 2019.

[17] X. Tong *et al.*, "Increased vegetation growth and carbon stock in China karst via ecological engineering," *Nature Sustainability*, vol. 1, no. 1, pp. 44–50, Jan. 2018.

[18] M. C. Vecchio, V. A. Bolaños, R. A. Golluscio, and A. M. Rodríguez, "Rotational grazing and exclosure improves grassland condition of the halophytic steppe in Flooding Pampa (Argentina) compared with continuous grazing," *Rangel. J.*, vol. 41, no. 1, pp. 1–12, 2019.

[19] T. Dvořáková Březinová and J. Vymazal, "Evaluation of macrophytes suitable for agriculture drainage treatment with respect to their carbon sequestration potential," *Ecol. Eng.*, vol. 124, pp. 31–37, Dec. 2018.

[20] X. Lu, X. Lu, and Y. Liao, "Conservation tillage increases carbon sequestration of winter wheat-summer maize farmland on Loess Plateau in China," *PLoS ONE*, vol. 13, no. 9, Sep. 2018, Art. no. e0199846.

[21] B. Belay, E. Pötzelsberger, and H. Hasenauer, "The carbon sequestration potential of degraded agricultural land in the Amhara region of Ethiopia," *Forests*, vol. 9, no. 8, p. 470, Aug. 2018.

[22] N. Ghasemi, M. R. Sahebi, and A. Mohammadzadeh, "Biomass estimation of a temperate deciduous forest using wavelet analysis," *IEEE Trans. Geosci. Remote Sens.*, vol. 51, no. 2, pp. 765–776, Feb. 2013.

[23] C. Gang *et al.*, "Quantitative assessment of the contributions of climate change and human activities on global grassland degradation," *Environ. Earth Sci.*, vol. 72, no. 11, pp. 4273–4282, Dec. 2014.

[24] S. Sannigrahi, "Modeling terrestrial ecosystem productivity of an estuarine ecosystem in the Sundarban biosphere region, India using seven ecosystem models," *Ecol. Model.*, vol. 356, pp. 73–90, Jul. 2017.

[25] J. T. Abatzoglou, S. Z. Dobrowski, S. A. Parks, and K. C. Hegewisch, "TerraClimate, a high-resolution global dataset of monthly climate and climatic water balance from 1958–2015," *Sci. Data*, vol. 5, no. 1, pp. 1–12, Jan. 2018.

[26] P. G. Jones and P. K. Thornton, "Representative soil profiles for the harmonized world soil database at different spatial resolutions for agricultural modelling applications," *Agricult. Syst.*, vol. 139, pp. 93–99, Oct. 2015.

[27] X. Guan, H. Shen, X. Li, W. Gan, and L. Zhang, "Climate control on net primary productivity in the complicated mountainous area: A case study of Yunnan, China," *IEEE J. Sel. Topics Appl. Earth Observ. Remote Sens.*, vol. 11, no. 12, pp. 4637–4648, Dec. 2018.

[28] J. Iwahashi and R. J. Pike, "Automated classifications of topography from DEMs by an unsupervised nested-means algorithm and a three-part geometric signature," *Geomorphology*, vol. 86, nos. 3–4, pp. 409–440, May 2007.